

Optimal Planning for Introducing Hydrogen Systems in a Multi-node Smart Grid

Charalampos Galatsopoulos^{a,*}, Simira Papadopoulou^b, Chrysovalantou Ziogou^a, Dimitris Trigkas^a, Spyros Voutetakis^a

^aChemical Process and Energy Resources Institute (CPERI), Centre for Research and Technology Hellas (CERTH), P.O. Box 60361, 57001 Thessaloniki, Thessaloniki, Greece

^bDepartment of Automation Engineering, Alexander Technological Educational Institute of Thessaloniki, P.O. Box 141, 54700 Thessaloniki, Greece
cgalatso@cperi.certh.gr

In this work, the optimal planning for introducing hydrogen technologies in a multi-node smart grid and the optimal operation for those hydrogen systems are discussed. In a multi-node grid with Renewable Energy Sources (RES), the energy production, storage and consumption might differ significantly from node to node, especially if the distances between the nodes are notably long. Consequently, this might lead to considerable energy surplus in some locations of the grid and energy deficit in others. In order to overcome these undesirable phenomena two tools are developed. The first tool explores the potential of introducing hydrogen production systems in each node of the grid separately by taking into account various parameters such as energy profiles and economic criteria. The second tool determines the optimal operation scheduling for the electrochemical devices (Fuel Cells) that process the produced H₂. Indicative results of both tools are presented so as to demonstrate the benefits of introducing hydrogen technologies to the grid.

1. Introduction

Nowadays, the development of multi-node smart grids with renewable energy sources (RES) is on the rise. In many cases multiple RES are used and also various energy storage technologies such as batteries, hydrogen through photocatalytic water splitting, hydrogen through bio-catalysed electrolysis etc. Utilizing a combination of miscellaneous sources can result to the delivery of power in a reliable and efficient way (Hosseinzadeh et al., 2013). Therefore, utilizing both batteries and fuel cells in hybrid energy stations (Ziogou et al., 2016) is an ordinary case. The objective of the optimal planning is to determine an efficient solution for exploiting the energy surplus. Maximizing the hydrogen storage from the unused energy which is produced from the RES, yield to multiple benefits. First and foremost, the determination of high hydrogen storage capabilities proves the value of installing high-powered Fuel Cells (FC) in nodes where energy deficit is observed frequently. Furthermore, high hydrogen storage outcomes the reduction of energy exchange between the nodes. Losses during transmission can reach 4% of the generated power (Chen et al., 1977). Thus, minimizing the energy exchange between the nodes is of great importance since it decreases the energy losses which are occurred during transmission. In addition, installation of high-powered FCs provides the option of disengaging the Battery Energy Storage Systems (BESS) of the node for a period of time per day or reducing the charging/discharging rates. This can be deemed crucial since heavy workload of a BESS (deep depth of discharges and high currents) results to massive damage at the batteries (Galatsopoulos et al., 2018). Therefore, by introducing a high-powered FC, the ageing effects at the node's BESS are decreased. Utilization of the stored hydrogen in an efficient way is equally important with the optimal design for maximizing hydrogen production and storage. In a grid where the pivotal role for load covering belongs to RES and BESS of each node, this implies the capability of using the FCs in an efficient way so as to increase their lifetime expectancy. Dynamic Programming (DP) and Model Predictive Control (MPC) (Ziogou et al., 2018) strategies can be applied to FCs in order to secure efficient and economic operation.



Figure 1: Optimal planning of electrolyzers' installation

The purpose of this work is the development of two simulation tools which will provide to the facilities manager of a multi-node smart grid the ability of exploring the potentiality of hydrogen technologies introduction to the grid. The first tool defines an optimal combination of electrolyzer devices for each node of the grid in order to maximize the hydrogen production and storage. The second tool determines the optimal operation scheduling for the FCs so as to guarantee high load covering and maintain their lifetime expectancy.

2. Optimal planning for introducing hydrogen systems

The optimal design simulation tool (Figure 1) proposes the planning for introducing hydrogen production systems to the grid and is implemented by applying a Mixed Integer Linear Programming (MILP) technique. The tool has the ability to perform linear optimization in up to five nodes of the grid simultaneously. The mandatory input data which must be set to the tool by the end user are: a) the power profile for each one of the nodes, b) the available budget for each node, c) the rated power of each electrolyzer's device and d) the corresponding price. By utilizing the aforementioned inputs the optimal design tool defines an optimal combination of the available electrolyzer devices for each node in order to guarantee high hydrogen production. Moreover, considering the optimal combination of the electrolyzers for each node and the relative forecasted profiles, a hydrogen consumption constraint is determined and feedforwarded to the Dynamic Programming simulation tool. The objective function of the MILP is stated as:

$$\min_{\{x_{ij}\}} f(x) = x_{1j} \cdot ED_{1pr} + x_{2j} \cdot ED_{2pr} + x_{3j} \cdot ED_{3pr} + x_{4j} \cdot ED_{4pr} \quad (1)$$

$$\text{s.t. } x_{1j} \cdot ED_{1pr} + x_{2j} \cdot ED_{2pr} + x_{3j} \cdot ED_{3pr} + x_{4j} \cdot ED_{4pr} \leq AB_j \text{ for } j = 1, 2, 3, 4, 5 \quad (2)$$

$$x_{1j} \cdot ED_1 + x_{2j} \cdot ED_2 + x_{3j} \cdot ED_3 + x_{4j} \cdot ED_4 \geq E_{min,j} \text{ for } j = 1, 2, 3, 4, 5 \quad (3)$$

where $x_{i,j}$ symbolizes the number of electrolyzer devices, j the number of the node, $ED_{i,pr}$ the corresponding price of each device, ED_i the relative rated power AB_j the available budget and $E_{min,j}$ the minimum energy which must be exploited for hydrogen production for each node respectively. In addition, the hydrogen consumption constraint is calculated by Eq (4) and Eq (5).

$$H_{2,max} = \sum_{i=1}^N n_{H2,i} \text{ for } i = 1, \dots, N \quad (4)$$

$$n_{H2} = n_f n_c I_{elec} / n_e F \quad (5)$$

where $n_{H2,i}$ denotes the hydrogen flow rate in mol/s at each time interval of electrolyzer's operation, n_c the number of cells, F the Faraday constant, n_f the Faraday efficiency, I_{elec} the electrolyzer's current and n_e the number of transferred electrons ($n_e=2$).

3. Dynamic programming of the fuel cells

The DP software simulation tool provides the capability of performing multiple simulation tests for the operation of Proton Exchange Membrane Fuel Cells (PEM FC) in order to prove their efficiency and lifetime expectancy before install them. The tool comprises the DP and the process that depicts its real operation. DP consists of the optimizer and the Prediction Model. A non-optimal operation profile is defined and an optimal profile is calculated. The non-optimal profile considers a forecasted energy profile and FC specifications.

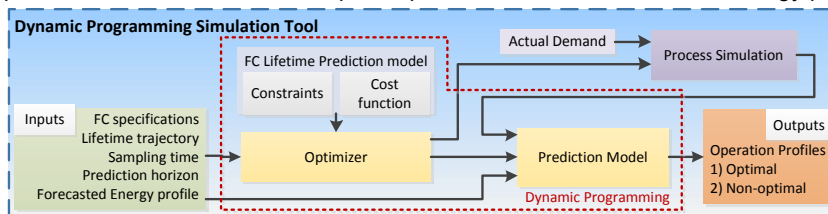


Figure 2: Dynamic Programming of PEM FC

The optimal profile provides an optimized operation of the PEM FC by utilizing the aforementioned inputs and a desirable lifetime trajectory. The widely used parametric FC model which is used by the tool comprises a combination of mechanistic and empirical relations with the I-V characteristic stated as (Amphlett et al., 1995):

$$V_{cell} = E - \eta_{act} - \eta_{ohmic} - \eta_{conc} \quad (6)$$

$$E = 1.229 - 0.85 \cdot 10^{-3} (T - 289.15) + 4.3085 \cdot 10^{-5} T (\ln P_{H_2} + 0.5 \ln P_{O_2}) \quad (7)$$

$$\eta_{act} = \xi_1 + \xi_2 T + \xi_3 T \ln(C_{O_2}) + \xi_4 T \ln(i) \quad (8)$$

$$C_{O_2} = P_{O_2} / 5.08 \cdot 10^{-6} e^{-498/T} \quad (9)$$

$$\eta_{ohmic} = i (\xi_5 + \xi_6 T + \xi_7 i) \quad (10)$$

$$\eta_{conc} = \xi_8 e^{i \xi_9} \quad (11)$$

$$H_{2,g} = nI / 2Fn_F \quad (12)$$

where E , n_{act} , n_{ohmic} and n_{conc} represent the thermodynamic voltage, the activation overvoltage, the ohmic overvoltage and the concentration overvoltage in V correspondingly, T symbolizes the operating temperature in K, P_{H_2} and P_{O_2} the partial pressures of hydrogen and oxygen in atm, ξ_i the constant parametric coefficients which are evaluated by experimental data, i the current density in A/cm², C_{O_2} denotes the concentration of the dissolved oxygen at the gas-liquid interface in mol/cm³, $H_{2,g}$ the hydrogen consumption rate, n the number of cells and I the FC's current. Furthermore, a lifetime prediction model (Chen et al., 2015) is utilized in order to define the cost function and the constraints to the optimizer.

$$L_{FC} = (\Delta V / N_{cells}) / k \cdot (c_{on/off} V_1 + t_{idling} U_1 + m_a V_2 + t_{rated} U_2) \quad (13)$$

Where L_{FC} represents the estimated FC lifetime, ΔV the maximum permissible voltage degradation value, k a constant factor, $c_{on/off}$ the average start-stop cycles per hour, V_1 the voltage degradation rate of each start-stop cycle in $\mu V/cycle$, t_{idling} the average idling time in min/h, U_1 the voltage degradation rate of idling operation in $\mu V/min$, m_a the average mode alternations per hour, V_2 the voltage degradation rate of each mode change in $\mu V/cycle$, t_{rated} the average rated power operation time in min/h, U_2 the voltage degradation rate of the high power load in $\mu V/min$. The non-optimal profile is defined simply by comparing the rated current of the PEM FC with the quotient of the division of the energy demand and the rated voltage. When the quotient is greater or equal to the rated current, the FC is set to operate at rated power. When is lower than the rated current and greater or equal to the idling current idling operation is set. Finally, if the quotient is lower than the idling current or the hydrogen consumption limit ($H_{2,cons_max}$) has been overreached the FC shuts down.

$$I_{FC(j)} = \begin{cases} 0, & \text{if } I_{FC_idling} > E_{D(j)} / V_{rated} \text{ or } \sum_{i=1}^{j-1} H_{2_cons(i)} > H_{2_cons_max} \\ I_{FC_idling}, & \text{if } I_{FC_idling} \geq E_{D(j)} / V_{rated} \text{ and } I_{FC_rated} < E_{D(j)} / V_{rated} \\ I_{FC_rated}, & \text{if } I_{FC_rated} \geq E_{D(j)} / V_{rated} \end{cases} \quad (14)$$

The dynamic optimization aims to minimize the deviation between the lifetime set point (L_{FC_sp}) and the actual lifetime (L_{FC}) of the FC which is estimated by Eq (13). This is achieved by designating optimal maximum limits for the FC's start/stop cycles ($c_{on/off}$), the operating minutes of each mode (t_{idling} , t_{rated}) and the alternations between the two modes (m_a). The objective function is stated as:

$$\min_{\{c_{on/off}, t_{idling}, m_a, t_{rated}\}} J = (L_{FC_sp} - L_{FC})^2 \quad (15)$$

$$\text{s.t. } c_{on/off} \leq c_{on/off_max} \quad (16)$$

$$t_{idling} \leq t_{idling_max} \quad (17)$$

$$m_a \leq m_{a_max} \quad (18)$$

$$t_{rated} \leq t_{rated_max} \quad (19)$$

$$\text{if } \sum_{i=1}^M H_{2_cons(i)} \leq H_{2_cons_max} \Rightarrow c_{on/off_{M+1}} = 0, t_{idling_{M+1}} = 0, m_{a_{M+1}} = 0, t_{rated_{M+1}} = 0 \quad (20)$$

Where M denotes the total number of past steps of the prediction horizon. The decision variables ($c_{on/off}$, t_{idling} , m_a , t_{rated}) must never exceed the corresponding maximum limits as this will signify that the optimizer proposes an infeasible solution. The limits are determined based on the length of the prediction horizon (e.g. if horizon=0.5 h and sampling time is 1 min, $m_{a_max}=29$). The optimal operation is designated according to Eq (22). If the needed current is greater or equal to I_{FC_rated} then I_{FC_opt} can be either I_{FC_rated} , I_{FC_idling} or 0 according to the values of the limits defined by the DP ($t_{rated(k)}$ and $t_{idling(k)}$). Likewise, if the needed current is lower than I_{FC_rated} and greater than I_{FC_idling} then I_{FC_opt} can be either I_{FC_idling} or 0.

$$I_{FC_opt(i)} = \begin{cases} I_{FC_rated}, & \text{if } I_{FC_rated} \geq E_{D(i)}/V_{rated} \text{ and } \sum_{i=1}^{j-1} t_{rated_c(i)} < t_{rated(i)} \\ I_{FC_idling}, & \text{if } I_{FC_rated} \geq E_{D(i)}/V_{rated} \text{ and } \sum_{i=1}^{j-1} t_{rated_c(i)} \geq t_{rated(i)}, \quad \sum_{i=1}^{j-1} t_{idling_c(i)} < t_{idling(i)} \\ 0, & \text{if } I_{FC_rated} \geq E_{D(i)}/V_{rated} \text{ and } \sum_{i=1}^{j-1} t_{rated_c(i)} \geq t_{rated(i)}, \quad \sum_{i=1}^{j-1} t_{idling_c(i)} \geq t_{idling(i)} \\ I_{FC_idling}, & \text{if } I_{FC_idling} \geq E_{D(i)}/V_{rated} \text{ and } \sum_{i=1}^{j-1} t_{idling_c(i)} < t_{idling(i)} \\ 0, & \text{if } I_{FC_idling} \geq E_{D(i)}/V_{rated} \text{ and } \sum_{i=1}^{j-1} t_{idling_c(i)} \geq t_{idling(i)} \\ 0 & \text{if } I_{FC_idling} \geq E_{D(i)}/V_{rated} \text{ or } \sum_{i=1}^{j-1} H_{2_cons(i)} > H_{2_cons_max} \end{cases} \quad (22)$$

Where t_{rated_c} , t_{idling_c} are relative counters of the past values of t_{rated} and t_{idling} . In order to simulate the optimal operation of a FC various input parameters must be set to the DP simulation tool. First of all, specifications for the FC such as temperature, number of cells, permitted voltage degradation, voltage at rated operation, partial pressure of H_2 , FC model's (Amphlett et al., 1995) constant parametric coefficients, idling operation current and rated operation current. Moreover, the DP needs to retrieve the FC's lifetime set point, the energy consumption profile, the sampling time and the prediction horizon. In the following simulated scenario the specifications of the evaluated with experimental data FC model FCS-C3000 are set. The rated power of the above-mentioned model is 3,000 W. It comprises 72 cells, generates up to 68.4 V and at maximum power produces 43.2 V (which implies $I_{FC_rated} = 70$ A). The idling current is set to 10 A. Furthermore, the FC operating temperature is 45°C, the partial pressure of hydrogen is 0.5 bar and the permitted FC voltage degradation 25 V (0.3472 V per cell). In addition, the constant parametric coefficients are displayed in table 1. The prediction horizon is set to 30 min, sampling time to 1 min and the lifetime trajectory to 2,500 h.

Table 1: PEM FC's constant parametric coefficients

ξ_1	ξ_2	ξ_3	ξ_4	ξ_5	ξ_6	ξ_7	ξ_8	ξ_9
29.12	-2.886	$5.84 \cdot 10^{-5}$	-0.18	0.507	-0.0016	$1.87 \cdot 10^{-5}$	$2.45 \cdot 10^{-5}$	0.112

4. Simulation Results and Discussion

4.1 Optimal design simulation tool

Primarily, the optimal design simulation tool is tested so as to define the planning of the electrolyzers' installation to specific nodes of the grid. Thereafter, the hydrogen consumption limit is calculated and feedforwarded to the DP tool. The power excess profiles and the relative available budgets for five nodes of the grid (node 1: 550 k€, node 2: 450 k€, node 3: 650 k€, node 4: 500 k€ and node 5: 550 k€) are provided to the optimal design simulation tool. Moreover, the rated power and the corresponding price for each electrolyzer are set (electrolyzer 1: 1 kW, 10 k€, electrolyzer 2: 2 kW, 18 k€, electrolyzer 3: 5 kW, 45 k€ and electrolyzer 4: 10 kW, 79 k€). Last but not least, the end user sets the minimum amount of energy surplus which must be exploited by the optimal combination of electrolyzers at each node. Thereupon, the MILP determines the optimal solution for each one of the five nodes (Figure 3).

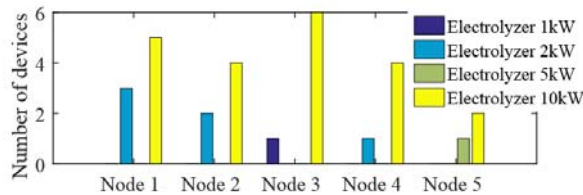


Figure 3: MILP output

Once the MILP defines the optimal solution for the electrolyzers' installation, the end user has the option to calculate the maximum amount of hydrogen to be produced at each location for specific periods of time by applying to the tool various expected energy profiles. The average produced hydrogen of all the simulated scenarios is feedforwarded to the DP tool to be used as a hydrogen consumption limit. Nevertheless, the end user has the option to set manually the limit to the DP.

4.2 Dynamic programming simulation tool

In the dynamic programming tool, except of the hydrogen consumption limit a forecasted power demand profile (Figure 4a) is considered. In addition, in Figure 4b the relative needed operating currents for the PEM FC in order to cover the whole power demand are displayed. By utilizing Eq (15) the non-optimal predictive operation schedule is defined at each step of the prediction horizon. At the end of the horizon Figure 6 is obtained by process simulation and displays the actual non-optimal operation schedule. It is observed that FC

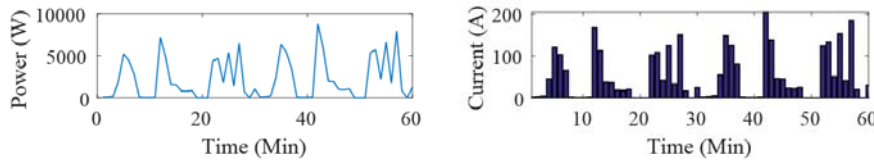


Figure 4a: Forecasted power demand profile Figure 4b: corresponding currents

operates for 8 min in rated mode and for 11 min in idling mode. Additionally, the alternations between idling and rated operation are 8 and the switch on/off cycles 4. By utilizing the optimizer, the DP decision variables are redefined at each step of the horizon (Figure 6) by taking into account updates at the forecasted energy profile. The decision variables represent optimal maximum limits of $c_{on/off}$, t_{idling} , m_a and t_{rated} for the whole prediction horizon. The process simulation defines the operation of the PEM FC at the present step, keeps a record of past values and feeds these values to the DP. At the end of the horizon the optimal operation of the

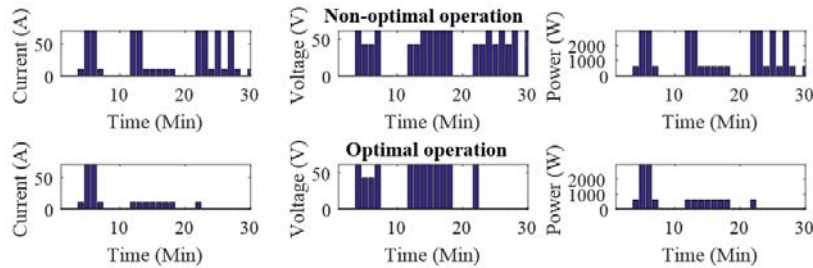


Figure 5: Non-optimal and optimal operation of the PEM FC

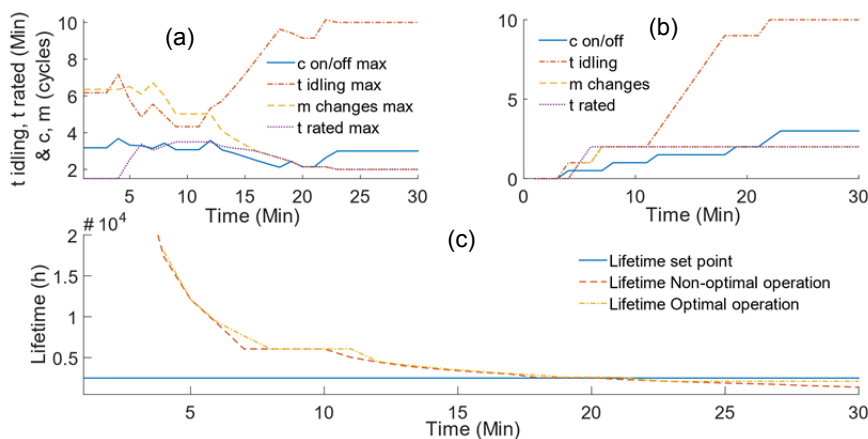


Figure 6: a) optimal max limits, b) actual values, c) DP output

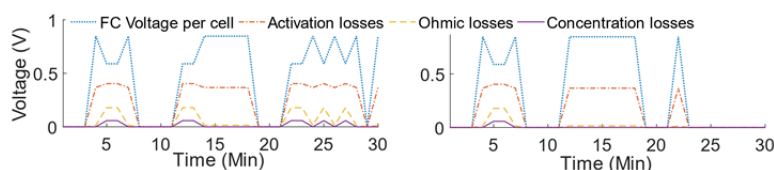


Figure 7: PEM FC losses for non-optimal (left) and optimal operation (right)

FC is obtained (Figure 5). It is observed that FC operates for 2 min in rated mode and for 10 min in idling mode. Furthermore, the mode alterations are 2 and the switch on/off cycles as well. Comparing the two operation profiles it is noted that the optimizer replaced 3 minutes of rated operation with idling operation and switched off the FC at step 22 until the end of the horizon so as to reduce the degradation effects. The achieved lifetime (2,213 h) is slightly lower than the desired one (2,500 h) and significantly higher than the estimated one during the non-optimal operation (1,381 h). Lastly, the DP simulation tool calculates and displays (Figure 7) the voltage losses for both optimal and non-optimal operation schedule of the FC.

5. Conclusions

Introducing different types of energy storage in a multi-node grid is a quite appealing solution for improving grid's efficiency. This is due to the ability of exploiting the advantages of each type of energy storage. In this work, optimization methodologies are presented in order to facilitate the decision of importing hydrogen technologies to a grid. Initially, a MILP based methodology is presented so as to define the optimal planning for installation of hydrogen production systems in multiple nodes based on various technical and economic criteria. Afterwards, a DP methodology is presented in order to demonstrate the optimal operation of PEM FCs in the grid based on day-ahead energy demand profiles, on available amount of hydrogen for consumption and on degradation constraints. The simulation results prove the capability of the MILP technique to provide an optimal planning for future installation of electrolyzers in specific nodes of the grid with respect to the criteria set by the end user. Similarly, it is concluded that the DP manages to define an optimal predictive operation schedule for the PEM FC according to the specifications and constraints set. More specifically, it is achieved to increase the lifetime expectancy of the FC by 832 h. Summing up, the demonstration of the aforementioned optimization methodologies proves their utility by providing valuable conclusions to the end user regarding the possible future introduction of hydrogen technologies in a grid so as to reduce the energy exchange between the nodes and the operating hours of the already installed BESSs.

Acknowledgments

Research supported by EU funded HORIZON2020 project inteGRIDy - integrated Smart GRID Cross-Functional Solutions for Optimized Synergetic Energy Distribution, Utilization & Storage Technologies, H2020 Grant Agreement Number: 731268.

References

- Amphlett J., Baumert R., Mann R., Peppley B., 1995, Performance Modeling of the Ballard Mark IV Solid Polymer Electrolyte Fuel Cell, *Journal of the Electrochemical Society*, 142, 1-8.
- Chen M.S., Ohba Y., Reynolds L. G., Dickson W.D., 1977, Losses in electrical power systems, *Electric Power Systems Research*, 1, 9-19.
- Chen H., Pei P., Song M., 2015, Lifetime prediction and the economic lifetime of Proton Exchange Membrane fuel cells, *Applied Energy*, 142, 154-163.
- Galatsopoulos C., Papadopoulou S., Ziogou C., Trigkas D., Yfoulis C., Voutetakis S., 2018, Non-Linear Model Predictive Control for Preventing Premature Aging in Battery Energy Storage System, *International Conference on Control (CONTROL-18)*, 5-7 Sept.2018, Sheffield, United Kingdom.
- Hosseinzadeh E., Rokni M., Advani S. G., Prasad A. K., 2013, Performance simulation and analysis of a fuel cell/battery hybrid forklift truck, *International Journal of Hydrogen Energy*, 38, 4241-4249.
- Ziogou C., Giaouris D., Papadopoulou S., Voutetakis S., 2016, Supervisory Control and Monitoring of a Hybrid High Temperature PEM Fuel Cell System with Li-Ion Batteries and an LPG Reformer, *Chemical Engineering Transactions*, 52, 1021-1026.
- Ziogou C., Voutetakis S., Georgiadis M., Papadopoulou S., 2018, Model Predictive Control (MPC) strategies for PEM fuel cells systems – A comparative experimental demonstration, *Chemical Engineering Research and Design*, 131, 656-670.